Facile Decoration of Functionalized Single-Wall Carbon Nanotubes with Phthalocyanines via 'Click Chemistry'

ARTICLE *in* JOURNAL OF THE AMERICAN CHEMICAL SOCIETY · AUGUST 2008

Impact Factor: 12.11 · DOI: 10.1021/ja8033262 · Source: PubMed

J|A|C|S
ARTICLES

Published on Web 07/29/2008

Facile Decoration of Functionalized Single-Wall Carbon Nanotubes with Phthalocyanines via "Click Chemistry"

Stéphane Campidelli,*,† Beatriz Ballesteros,‡ Arianna Filoramo,† David Díaz Díaz,‡ Gema de la Torre,‡ Tomás Torres,*,‡ G. M. Aminur Rahman,§ Christian Ehli,§ Daniel Kiessling,§ Fabian Werner,§ Vito Sgobba,§ Dirk M. Guldi,*,§ Carla Cioffi,# Maurizio Prato,# and Jean-Philippe Bourgoin†

Laboratoire d'Electronique Moléculaire, DSM/IRAMIS/SPEC (CNRS URA 2464), CEA Saclay, F-91191 Gif sur Yvette Cedex, France, Departamento de Química Orgánica, Universidad Autónoma de Madrid, Cantoblanco, E-28049 Madrid, Spain, Department of Chemistry and Pharmacy & Interdisciplinary Center for Molecular Materials, Friedrich-Alexander-Universität Erlangen-Nürnberg, Egerlandstrasse 3, D-91058 Erlangen, Germany, and INSTM, Unit of Trieste, Dipartimento di Scienze Farmaceutiche, Università di Trieste, Piazzale Europa, 1, I-34127 Trieste, Italy

Received May 5, 2008; E-mail: stephane.campidelli@cea.fr; tomas.torres@uam.es

Abstract: We describe the functionalization of single-wall carbon nanotubes (SWNTs) with 4-(2-trimethylsilyl)ethynylaniline and the subsequent attachment of a zinc-phthalocyanine (ZnPc) derivative using the reliable Huisgen 1,3-dipolar cycloaddition. The motivation of this study was the preparation of a nanotube-based platform which allows the facile fabrication of more complex functional nanometer-scale structures, such as a SWNT−ZnPc hybrid. The nanotube derivatives described here were fully characterized by a combination of analytical techniques such as Raman, absorption and emission spectroscopy, atomic force and scanning electron microscopy (AFM and SEM), and thermogravimetric analysis (TGA). The SWNT−ZnPc nanoconjugate was also investigated with a series of steady-state and time-resolved spectroscopy experiments, and a photoinduced communication between the two photoactive components (i.e., SWNT and ZnPc) was identified. Such beneficial features lead to monochromatic internal photoconversion efficiencies of 17.3% when the SWNT−ZnPc hybrid material was tested as photoactive material in an ITO photoanode.

Introduction

Nanotechnologies actually represent a field that stimulates the imagination of many people (not only scientists but also economists and sociologists) for the development of new materials with new structures, functionalities, and applications.[1–3] Carbon nanotubes (CNTs)[4–6] constitute a relatively new class of nanostructures composed exclusively of carbon atoms. Because of their electronic and mechanical properties, carbon nanotubes appear to be promising materials for polymer composites,[7–10] energy conversion,[11–17] electronics and sensing,[18–20] or biological applications.[21–26] In particular, single-wall carbon nanotubes (SWNTs) are one-dimensional nanowires that are either metallic or semiconducting. They readily accept charges, which can then be transported under nearly ideal conditions along the tubular SWNT axis.[27,28] The electrical conductivity, morphology, and good chemical stability of SWNTs are promising features that stimulate their integration into photovoltaic systems or electronic devices.

† DSM/IRAMIS/SPEC (CNRS URA 2464) CEA Saclay.
‡ Universidad Autónoma de Madrid.
§ Friedrich-Alexander-Universität Erlangen-Nürnberg.
# Università di Trieste.

(1) Poole, C. P.; Owens, F. J. *Introduction to Nanotechnology*; Wiley-Interscience: Weinheim, Germany, 2003.
(2) Liz-Marzán, L. M.; Kamat, P. V. *Nanoscale Materials*; Springer: Berlin, Germany: 2003.
(3) Wolf, E. L. *Nanophysics and Nanotechnology: An Introduction to Modern Concepts in Nanoscience*; John Wiley and Sons: New York, 2004.
(4) Dresselhaus, M. S.; Dresselhaus, G.; Avouris, P. *Carbon Nanotubes: Synthesis, Structure, Properties, and Applications*; Springer-Verlag: Berlin, 2001.
(5) O'Connell, M. J. *Carbon Nanotubes: Properties and Applications*; CRC Press: Boca Raton, FL, 2006.
(6) Reich, S.; Thomsen, C.; Maultzsch, J. *Carbon Nanotubes: Basic Concepts and Physical Properties*; VCH: Weinheim, Germany, 2004.
(7) Harris, P. J. F. *Int. Mater. Rev.* **2004**, *49*, 31.
(8) Chae, H. G.; Sreekumar, T. V.; Uchida, T.; Kumar, S. *Polymer* **2005**, *46*, 10925.
(9) Miyagawa, H.; Misra, M.; Mohanty, A. K. *J. Nanosci. Nanotechnol.* **2005**, *5*, 1593.
(10) Baibarac, M.; Gómez-Romero, P. *J. Nanosci. Nanotechnol.* **2006**, *6*, 289.
(11) Guldi, D. M.; Rahman, G. M. A.; Zerbetto, F.; Prato, M. *Acc. Chem. Res.* **2005**, *38*, 871.
(12) Rahman, G. M. A.; Guldi, D. M.; Cagnoli, R.; Mucci, A.; Schenetti, L.; Vaccari, L.; Prato, M. *J. Am. Chem. Soc.* **2005**, *127*, 10051.
(13) Guldi, D. M.; Rahman, G. M. A.; Sgobba, V.; Kotov, N. A.; Bonifazi, D.; Prato, M. *J. Am. Chem. Soc.* **2006**, *128*, 2315.
(14) Landi, B. J.; Castro, S. L.; Ruf, H. J.; Evans, C. M.; Bailey, S. G.; Raffaelle, R. P. *Sol. Energy Mater. Sol. Cells* **2005**, *87*, 733.
(15) Raffaelle, R. P.; Landi, B. J.; Harris, J. D.; Bailey, S. G.; Hepp, A. F. *Mater. Sci. Eng. B* **2005**, *116*, 233.
(16) Bhattacharyya, S.; Kymakis, E.; Amaratunga, G. A. J. *Chem. Mater.* **2004**, *16*, 4819.

Scheme 1[a]

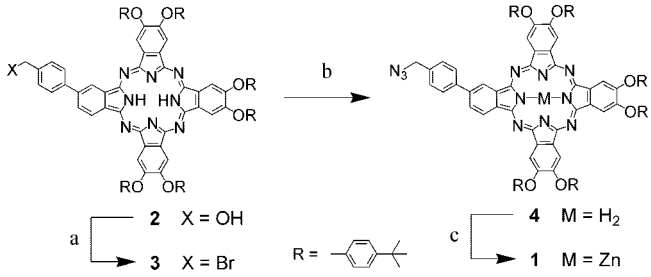

[a] (a) PBr_3, CH_2Cl_2, rt, 2 h, 85%; (b) NaN_3, THF/H_2O, 70 °C, 4 h, 82%; (c) $ZnCl_2$, chlorobenzene/DMF, 100 °C, 3 h, 88%.

However, fabrication of nanotube-based molecular assemblies is still limited because of the difficulty to incorporate highly engineered molecules on the nanotube surfaces. This problematic issue can have mainly two origins: incompatibility between the functionality on the molecules and the conditions required for nanotube functionalization and/or the fact that nanotube functionalization requires a large excess of reagent which is difficult or impossible to recycle. There is a real need for simple and versatile reactions that can easily lead to nanotube-based functional materials.

The emerging field of "click chemistry" can bring very elegant solutions to easily achieve nanotube-based functional materials.[29,30] The term "click chemistry"[31] defines a chemical reaction which is versatile and clean, with simple workup and purification procedures. Among the large collection of organic reactions, Huisgen cycloaddition, 1,3-dipolar cycloaddition between azide and acetylene derivatives in the presence of Cu(I) catalyst, represents the most effective reaction of "click chemistry".[32–35]

On the other hand, the attachment of phthalocyanines (Pcs) to nanotubes[36–38] and fullerenes[39–41] has recently emerged as an excellent approach to carbon nanostructure Pc-based photovoltaic and other electronic devices. Phthalocyanines are planar electron-rich aromatic macrocycles that are characterized by their remarkably high extinction coefficients in the red/near-infrared region (which is an important part of the solar spectrum) and their outstanding photostability and singular physical properties.[42–44] These features render them exceptional donor/antenna building blocks for their incorporation in photovoltaic devices.[45–49] The development of a suitable method to easily graft phthalocyanines or other photoactive species onto carbon nanotubes is thus an important objective toward the realization of materials with improved optoelectronic performances.

Here we describe the functionalization of SWNTs with 4-(trimethylsilyl)ethynylaniline following the procedure developed by Tour and co-workers[50] and the subsequent attachment of a zinc-phthalocyanine (ZnPc) derivative bearing an azide group. We show how the Huisgen cycloaddition reaction on functionalized nanotubes yields new nanotube-based molecular assemblies and overcomes the problems of functionalization of carbon nanotubes listed above. The resulting SWNT−ZnPc conjugate was fully characterized, and its photovoltaic properties were tested.

Results and Discussion

Synthesis. Synthesis of phthalocyanine **1** is depicted in Scheme 1. Bromination of metal-free phthalocyanine **2**[37] gave **3**, which was converted into **4** by reaction with sodium azide. Finally, addition of zinc chloride to **4** led to Zn(II) azidophthalocyanine **1**. The synthesis of the SWNT−ZnPc conjugate **5** is described in Scheme 2. The SWNT material used in the present work was produced via laser ablation technique by Dr. Oliver Jost (University of Dresden).[51] The raw material contains

(17) Ago, H.; Petritsch, K.; Shaffer, M. S. P.; Windle, A. H.; Friend, R. H. *Adv. Mater.* **1999**, *11*, 1281.
(18) Freitag, M. Carbon nanotube electronics and devices; In *Carbon Nanotubes: Properties and Applicatons*; O'Connell, M. J., Ed.; CRC Press: Boca Raton, FL, 2006; pp 83−117..
(19) Lee, M.; Im, J.; Lee, B. Y.; Myung, S.; Kang, J.; Huang, L.; Kwon, Y.-K.; Hong, S. *Nat. Nanotechnol.* **2006**, *1*, 66.
(20) Borghetti, J.; Derycke, V.; Lenfant, S.; Chenevier, P.; Filoramo, A.; Goffman, M.; Vuillaume, D.; Bourgoin, J.-P. *Adv. Mater.* **2006**, *18*, 2535.
(21) Katz, E.; Willner, I. *ChemPhysChem.* **2004**, *5*, 1084.
(22) Lin, Y.; Tailor, S.; Li, H.; Shiral Fernando, K. A.; Qu, L.; Wang, W.; Gu, L.; Zhou, B.; Sun, Y.-P. *J. Mater. Chem.* **2004**, *14*, 527.
(23) Bianco, A.; Kostaleros, K.; Partidos, C. D.; Prato, M. *Chem. Commun.* **2005**, 571.
(24) Kostaleros, K.; Lacerda, L.; Pastorin, G.; Wu, W.; Wieckowski, S.; Luangsivilay, J.; Godefroy, S.; Pantarotto, D.; Briand, J.-P.; Muller, S.; Prato, M.; Bianco, A. *Nat. Nanotechnol.* **2007**, *2*, 108.
(25) Kam, N. W. S.; O'Connell, M.; Wisdom, J. A.; Dai, H. *Proc. Natl. Acad. Sci. U.S.A.* **2005**, *102*, 11600.
(26) Kam, N. W. S.; Dai, H. *J. Am. Chem. Soc.* **2005**, *127*, 6021.
(27) Javey, A.; Guo, J.; Wang, Q.; Lundstrom, M.; Dai, H. *Nature* **2003**, *424*, 654.
(28) Latil, S.; Roche, S.; Charlier, J.-C. *Nano Lett.* **2005**, *5*, 2216.
(29) Li, H.; Cheng, F.; Duft, A. M.; Adronov, A. *J. Am. Chem. Soc.* **2005**, *127*, 14518.
(30) Nandivada, H.; Jiang, X.; Lahann, J. *Adv. Mater.* **2007**, *19*, 2197.
(31) Kolb, H. C.; Finn, M. G.; Sharpless, K. B. *Angew. Chem., Int. Ed.* **2001**, *40*, 2004.
(32) Huisgen, R. In *1,3-Dipolar Cycloaddition Chemistry*; Padwa, A., Ed.; Wiley: New York, 1984; p 1.
(33) Rostovtsev, V. V.; Green, L. G.; Fokin, V. V.; Sharpless, K. B. *Angew. Chem., Int. Ed.* **2002**, *41*, 2596.
(34) Tornøe, C. W.; Christensen, C.; Meldal, M. *J. Org. Chem.* **2002**, *67*, 3057.
(35) Bock, V. D.; Hiemstra, H.; van Maarseveen, J. H. *Eur. J. Org. Chem.* **2006**, 51.
(36) de la Torre, G.; Blau, W.; Torres, T. *Nanotechnology* **2003**, *14*, 765.
(37) Ballesteros, B.; Campidelli, S.; de la Torre, G.; Ehli, C.; Guldi, D. M.; Prato, M.; Torres, T. *Chem. Commun.* **2007**, 2950.
(38) Ballesteros, B.; de la Torre, G.; Ehli, C.; Rahman, G. M. A.; Agulló-Rueda, F.; Guldi, D. M.; Torres, T. *J. Am. Chem. Soc.* **2007**, *129*, 5061.
(39) Guldi, D. M.; Gouloumis, A.; Vázquez, P.; Torres, T.; Georgakilas, V.; Prato, M. *J. Am. Chem. Soc.* **2005**, *127*, 5811.
(40) de la Escosura, A.; Martínez-Díaz, M. V.; Guldi, D. M.; Torres, T. *J. Am. Chem. Soc.* **2006**, *128*, 4112.
(41) Bottari, G.; Olea, D.; Gómez-Navaro, C.; Zamora, F.; Gómez-Herrero, J.; Torres, T. *Angew. Chem., Int. Ed.* **2008**, *47*, 2026.
(42) McKeown, N. B. *Phthalocyanine Materials: Synthesis, Structure and Function*; Cambridge University Press: Cambridge, 1998.
(43) de la Torre, G.; Vázquez, P.; Agulló-López, F.; Torres, T. *Chem. Rev.* **2004**, *104*, 3723.
(44) de la Torre, G.; Claessens, C. G.; Torres, T. *Chem. Commun.* **2007**, 2000.
(45) Palomares, E.; Martinez-Diaz, M. V.; Haque, S. A.; Torres, T.; Durrant, J. R. *Chem. Commun.* **2004**, 2112.
(46) Morandeira, A.; Lopez-Duarte, I.; Martinez-Diaz, M. V.; O'Regan, B.; Shuttle, B.; Haji-Zainulabidin, N. A.; Torres, T.; Palomares, E.; Durrant, J. R. *J. Am. Chem. Soc.* **2007**, *129*, 9250.
(47) Reddy, P. Y.; Giribabu, L.; Lyness, C.; Snaith, H. J.; Vijaykumar, C.; Chandrasekharam, M.; Lakshmikantam, M.; Yum, J.-H.; Kalyanasundaram, K.; Graetzel, M.; Nazeeruddin, M. K. *Angew. Chem., Int. Ed.* **2007**, *46*, 373.
(48) Cid, J.-J.; Yum, J.-H.; Jang, S.-R.; Nazeeruddin, M. K.; Martinez-Ferrero, E.; Palomares, E.; Ko, J.; Graetzel, M.; Torres, T. *Angew. Chem., Int. Ed.* **2007**, *46*, 8358.
(49) O'Regan, B. C.; Lopez-Duarte, I.; Martinez-Diaz, M. V.; Forneli, A.; Albero, J.; Morandeira, A.; Palomares, E.; Torres, T.; Durrant, J. R. *J. Am. Chem. Soc.* **2008**, *130*, 2906.
(50) Bahr, J.; Tour, J. M. *Chem. Mater.* **2001**, *13*, 3823.
(51) Gorbunov, A. A.; Friedlein, R.; Jost, O.; Golden, M. S.; Fink, J.; Pompe, W. *Appl. Phys. A: Mater. Sci. Process.* **1999**, *69*, S593.

Scheme 2[a]

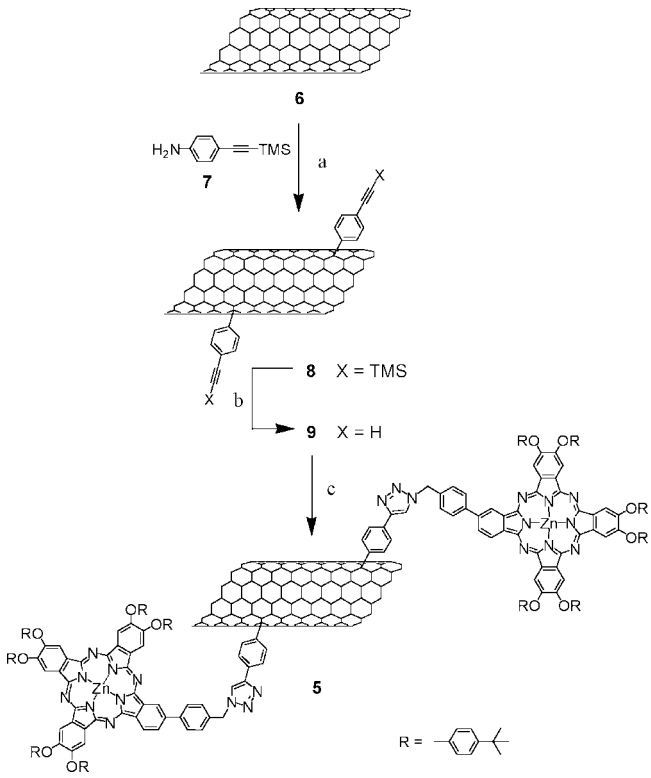

[a] (a) Isoamyl nitrite, NMP, 60 °C, 48 h; (b) NBu_4F, THF/NMP, rt, 1 h; (c) **1**, $CuSO_4 \cdot 5H_2O$, sodium ascorbate, NMP, 70 °C, 48 h.

approximately 60−70% of SWNTs and was purified by an optimized soft acidic treatment.[52] Reaction of purified SWNTs (*p*-SWNTs) **6** with 4-(2-trimethylsilyl)ethynylaniline **7**[53] in the presence of isoamyl nitrite in *N*-methylpyrrolidone (NMP) gave functionalized nanotubes (*f*-SWNTs) **8** which were deprotected by treatment with NBu_4F to give **9** and then allowed to react with azidophthalocyanine **1** in NMP in the presence of $CuSO_4$ and sodium ascorbate to give the nanotube-phthalocyanine assembly **5**.

As we explained before, the problematic issue of functionalization of carbon nanotubes is the excess of reagent generally involved in the reaction; functionalization of carbon nanotubes with diazonium derivatives required usually 4 equiv per carbon atom or more of amine precursor or diazonium salt.[50,54] Here for example, the functionalization of SWNTs with 4 equiv per carbon of 4-(2-trimethylsilyl)ethynylaniline is possible since this compound is synthesized very easily from 4-iodoaniline and ethynyltrimethylsilane; this kind of reaction cannot be envisioned with high added value molecules such as phthalocyanines: for example, the functionalization of 1 mg of SWNTs with 4 equiv per carbon atom of a hypothetical aminophenylphthalocyanine (containing an amino group linked directly on the phenyl group, see structure in Figure S1) *via* diazonium reaction would require 520 mg of phthalocyanine. However, two-step methods introduce more complexity, and they require the use of an efficient reaction, such as the Huisgen cycloaddition, for the final coupling.

Characterization. The nanotube derivatives were characterized by standard analytical techniques such as Raman,

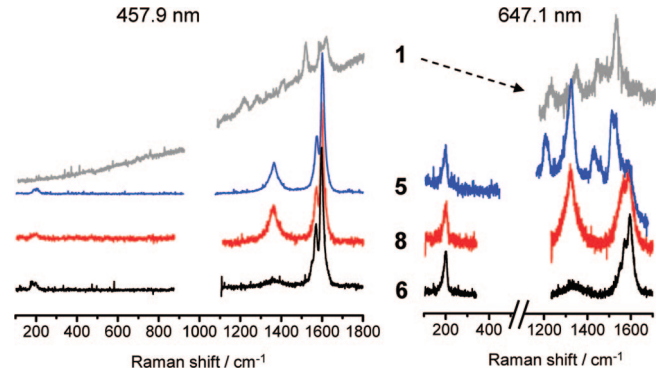

Figure 1. Raman spectra of the *p*-SWNTs **6** (black), *f*-SWNTs **8** (red), SWNT−ZnPc **5** (blue), and ZnPc **1** (gray) (excitation wavelength at 457.9 and 647.1 nm). The intensities have been normalized (for SWNT derivatives) with respect to the high frequency side of the G-band (ω_{G+}).

absorption and emission spectroscopy, atomic force and scanning electron microscopy (AFM and SEM), and thermogravimetric analysis (TGA). The Raman spectra of the *p*-SWNTs **6**, *f*-SWNTs **8**, SWNT−ZnPc conjugate **5**, and ZnPc **1** are shown in Figure 1. First of all, the Raman analysis of *p*-SWNTs **6** presented a very small D-band, indicating that most of the amorphous carbon was removed from the nanotube and that the acid treatment was soft enough to not damage the nanotubes. We do not observe any noticeable effect of the functionalization on the RBM and G-band features while we note a significant modification in the relative intensity of the D-band after the first functionalization step (*f*-SWNTs **8**). The metallic nanotubes (met-SWNTs), probed with excitation at 647.1 nm, present a higher functionalization compared to semiconducting tubes (sem-SWNTs) (probed with excitation at 457.9 nm, Figure 1). This behavior is in agreement with the fact that aryldiazonium derivatives react preferentially with metallic nanotubes.[55,56] After reaction with phthalocyanine **1**, the spectrum of SWNT−ZnPc **5**, obtained with excitation at 647.1 nm, presents new features that are attributed to the ZnPc chromophore, while the spectrum realized at 457.9 nm does not present important changes. This difference between the spectra of **5** can have two origins: (1) ZnPc absorbs strongly at 680 nm while it does not absorb around 450 nm, and the perturbation of the spectrum at 647.1 nm can be due to absorption and emission of the ZnPc moieties in **5**, and (2) met-SWNTs are more functionalized than sem-SWNTs (see Raman of **8**, red spectra in Figure 1); the latter would imply that after cycloaddition, the amount of ZnPc should be higher in met-SWNTs and so the response of phthalocyanine in the spectrum at 647.1 nm could be higher. However, the addition of phthalocyanine does not modify the linkage on the nanotube carbon lattice and the sp^2/sp^3 ratio as shown by the absence of change of the RBM and D-bands with respect to the G-band.

The thermogravimetric analysis showed a loss of weight of about 19% for *p*-SWNTs **6**, 27% for *f*-SWNTs **8**, 47% for SWNT−ZnPc **5**, and 43% for ZnPc **1** at 600 °C (Figure 2). The loss of weight observed for *p*-SWNTs between 200 and 600 °C may be due to the destruction of the residual amorphous

(52) Capes, L.; Valentin, E.; Esnouf, S.; Ribayrol, A.; Jost, O.; Filoramo, A.; Patillon, J.-N. *Proc. 2nd IEEE Conf. Nanotechnol.*, **2002**, 439.
(53) Hwang, J.-J.; Tour, J. M. *Tetrahedron* **2002**, *58*, 10387.
(54) Dyke, C. A.; Tour, J. M. *Nano Lett.* **2003**, *3*, 1215.
(55) Strano, M. S.; Dyke, C. A.; Ursey, M. L.; Barone, P. W.; Allen, M. J.; Shan, H. W.; Kittrell, C.; Hauge, R. H.; Tour, J. M.; Smalley, R. E. *Science* **2003**, *301*, 1519.
(56) Dyke, C. A.; Stewart, M. P.; Tour, J. M. *J. Am. Chem. Soc.* **2005**, *127*, 4497.

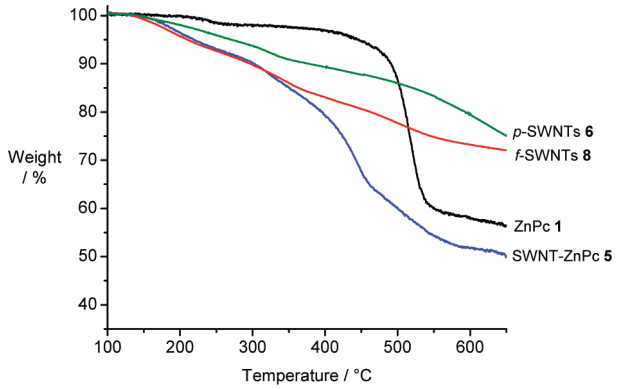

Figure 2. Thermogravimetric analysis of ZnPc **1** (black), *p*-SWNTs **6** (green), *f*-SWNTs **8** (red), and SWNT−ZnPc **5** (blue) (10 °C/min under N_2).

carbon still present in the nanotubes and to the decarboxylation of the oxidized species. The corrected weight losses due to the functional groups on nanotubes were then estimated to be 8% and 28% for *f*-SWNTs **8** and SWNT−ZnPc **5**, respectively (weight losses difference of *f*-SWNTs − *p*-SWNTs and SWNT−ZnPc − *p*-SWNTs). The number of phenylacetylene functional groups in **8** was then estimated as 1 per 165 carbon atoms.[57] With the same calculation (see ref 57), we estimated the amount of functional groups as 1 per 365 carbon atoms for SWNT−ZnPc **5**. This number does not represent the reality because at 600 °C the thermogram of ZnPc **1** presents a loss of weight of 43%. Considering that the weight loss corresponding to the clicked ZnPc is about 20% in SWNT−ZnPc **5** (SWNT−ZnPc − *f*-SWNTs), the amount of clicked ZnPc in **5** may correspond to a real ratio of *ca.* 47% (20%/43%). Then the number of functional groups in this case can be estimated to 1 phthalocyanine per 155 carbon atoms. Considering the error range of the TGA measurements, we can estimate a similar functionalization degree for *f*-SWNTs **8** and SWNT−ZnPc **5**. We believe that all the acetylenic groups have reacted with azidophthalocyanine moieties, thus pointing out the success of our approach.

The carbon nanotube derivatives have been investigated by AFM and SEM. The AFM pictures of *f*-SWNTs **8** and SWNT−ZnPc **5** (Figure 4) revealed the presence of individual or very thin bundles of nanotubes; the typical lengths of the objects are about 500 nm to 1.5 μm with diameters of about 1 to 3 nm. In SEM pictures of SWNT−ZnPc **5** (Figure 3), one can see the presence of nanotubes as spaghetti-like aggregates.

Absorption spectra of the nanotubes (performed in SDS/D_2O) are shown in Figure 5. The spectrum of functionalized nanotubes **8** presents a partial loss of the van Hove transitions compared to purified SWNTs. After cycloaddition, the spectrum of SWNT−ZnPc **5** shows two new maxima at 615 and 682 nm, which correspond to the Q-bands of the phthalocyanine. Considering the electron donor and electron acceptor character of ZnPc and SWNT, respectively, we tested the SWNT−ZnPc nanoconjugate **5** in a series of photophysical measurements. Fluorescence of the ZnPc **1** was compared to that of SWNT−ZnPc **5** suspended in THF solutions. Notably, the ZnPc-centered fluorescence is drastically quenched in SWNT−ZnPc **5** with quantum yields of 5.5×10^{-5} (compared to 0.3 for **1**, see Figure 6). Such efficient quenching implies a rapid deactivation of the photoexcited ZnPc. It is important to note in this context that the overall fluorescence pattern in the nanoconjugate **5** resembles that seen for the ZnPc **1**. In other words, despite being linked to SWNTs the ZnPc keep their electronic integrity.

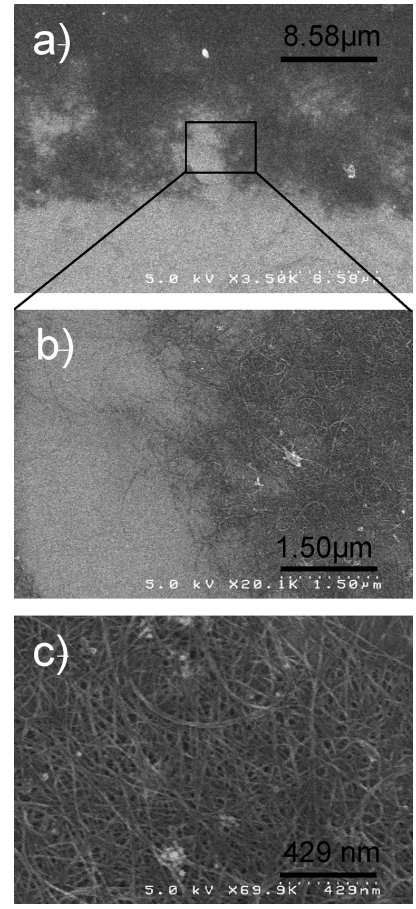

Figure 3. SEM pictures of SWNT−ZnPc **5**: (a) general view of the surface with nanotubes (dark gray); (b) close-up of the region delimited with the black rectangle; (c) picture taken at higher magnification in the center of the aggregate.

The fluorescence assays were complemented by transient absorption measurements to shed light on the photoproduct that is associated with the deactivation of the photoexcited ZnPc in SWNT−ZnPc **5**. In the ZnPc **1** the following changes occur upon 660 nm photoexcitation: the singlet excited state, which is formed essentially right after the laser pulse, comprises a broad transient maximum that is centered at 490 nm followed by bleaching between 610 and 685 nm (see Figure S2). This transient decays rather slowly on the time scale of our instrumental detection (i.e., 3.0 ns) by intersystem crossing to the corresponding triplet manifold. The main spectral feature of the latter is a maximum at 500 nm and a minimum at 680 nm. Implicit is that, especially in the near-infrared region, the two transients, namely, the singlet and the triplet excited state, differ largely in their absorption.

Looking at *p*-SWNTs **6**, which were simply suspended in THF, a set of transient minima was observed at 1050, 1185, 1310, 1435, and 1555 nm. As Figure S3 shows, all features decay similarly to recover the ground state with two major

(57) The weight loss was estimated using the following calculation: for example for *f*-SWNTs **8**, the amount of functional group is $(92/M_C)/(8/M_{\text{trimethylsilyl-phenylacetylene unit}}) = 165$; it means 1 group per about 165 carbon atoms.

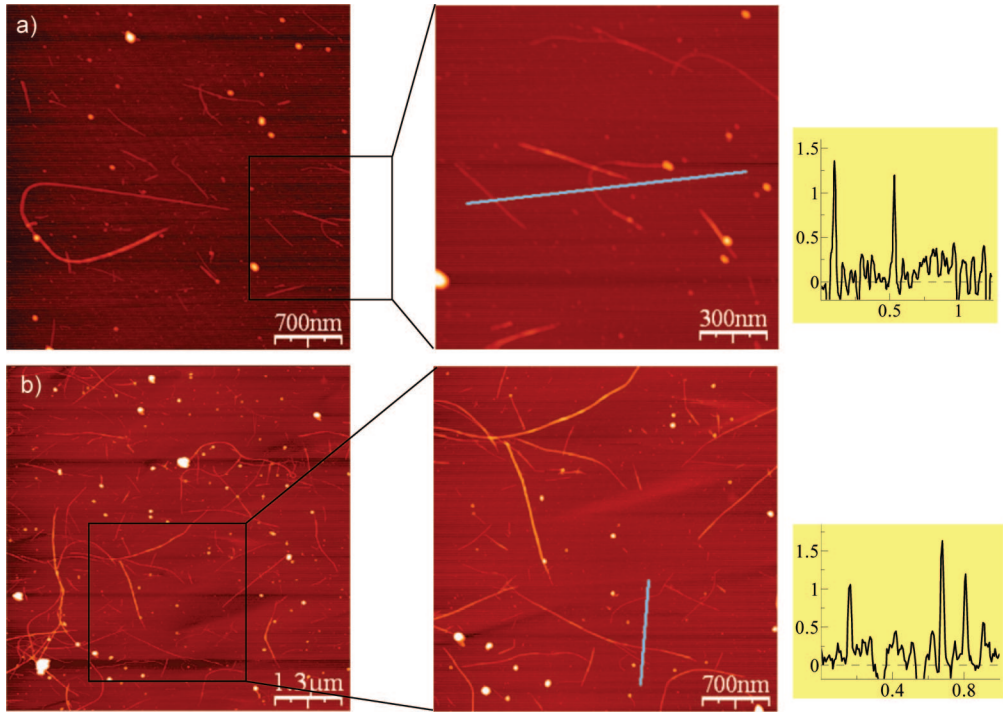

Figure 4. AFM pictures of *f*-SWNTs **8** (a) and SWNT−ZnPc **5** (b) on polylysine-coated mica. General view on the left with close-up of the surface and a line profile showing the height of the nanotubes on the middle and on the right.

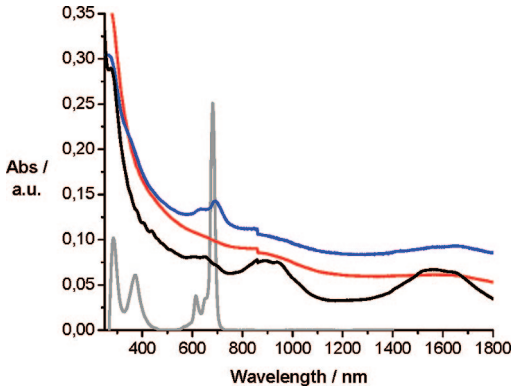

Figure 5. Absorption spectra of ZnPc **1** (gray) in NMP and *p*-SWNTs **6** (black), *f*-SWNTs **8** (red), and SWNT−ZnPc conjugates **5** (blue) in SDS (1.2 CMC)/ D_2O.

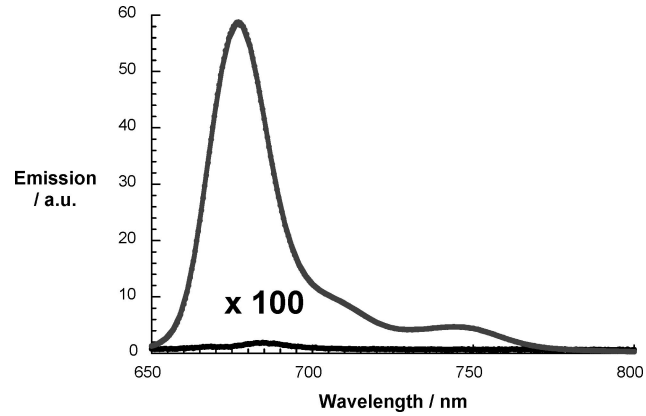

Figure 6. Steady-state fluorescence spectra of ZnPc reference (gray spectrum) and SWNT−ZnPc **5** (black spectrum) in THF at room temperature with matching absorption at the excitation wavelength (i.e., 650 nm). The spectra were not corrected for different ground state absorption at the excitation wavelength.

components (i.e., 1.2 and 520 ps), while no particular shifts were observable. In fact, this short-lived transient is a mirror image of the ground-state absorption, revealing a significant loss in oscillator strength upon excitation.

The same ZnPc singlet excited characteristics, despite the presence of the electron accepting SWNTs, were registered upon 660 nm photoexcitation of SWNT−ZnPc **5** (Figure 7 top). This confirms the successful excitation of the ZnPc component. In contrast to the slow intersystem crossing, which was noted for the ZnPc **1**, the ZnPc singlet excited-state features now decay rather quickly. The lifetimes (i.e., ∼20 ps) reflect the global trends seen in the fluorescence experiments (Figure 7, bottom). Simultaneously with the ZnPc singlet excited-state decay, the formation of a new transient species evolves with distinct maxima at 520 and 840 nm, which are attributes of the one-electron oxidized ZnPc radical cation. Similarly, the range beyond 1000 nm (i.e., 1000−1400 nm) is important, which immediately after the photoexcitation is dominated, for example in the case of SWNTs, by a negative imprint of the van Hove singularities. These spectral characteristics transform into a new product. Appreciable blue-shifts of the transient bleaches with minima that shift from 963 to 940 nm and from 1390 to 1335 nm are detected; see Figure 7. Implicit are new conduction band electrons, injected from ZnPc shifting the transitions to lower energies.[58]

Photovoltaic Properties. SWNTs, on one hand, and phthalocyanines, on the other hand, have been considered independently or together for PV applications, owing to their promising potential as electrodes or charge generation and separation

(58) Herranz, M. A.; Ehli, C.; Campidelli, S.; Gutiérrez, M.; Hug, G. L.; Ohkubo, K.; Fukuzumi, S.; Prato, M.; Martín, N.; Guldi, D. M. *J. Am. Chem. Soc.* **2008**, *130*, 66.

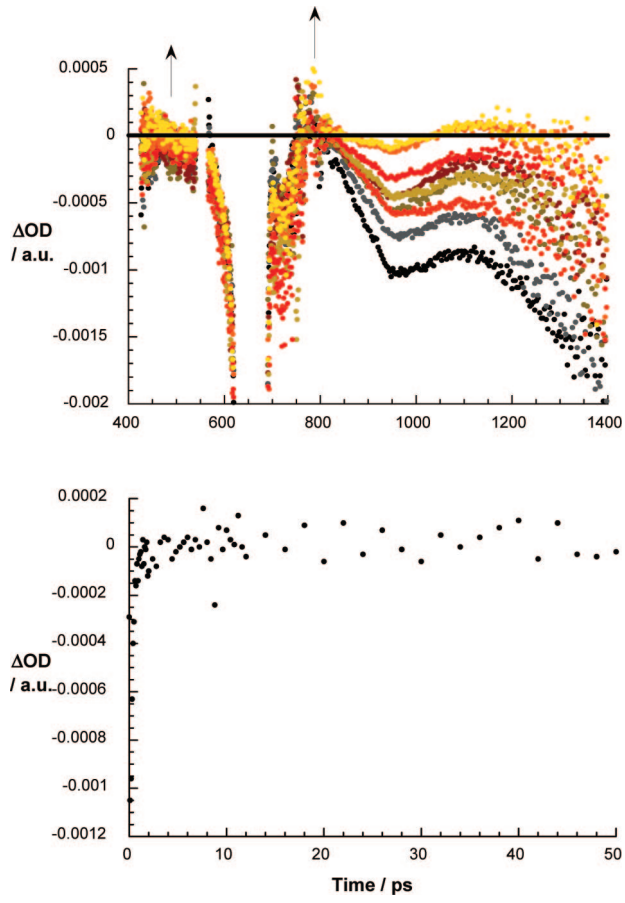

Figure 7. Upper part: differential absorption spectrum (near-infrared) obtained upon femtosecond flash photolysis (660 nm) of SWNT−ZnPc **5** in nitrogen-saturated THF with time delays between 0.5 ps (black spectrum) and 20 ps (yellow spectrum) at room temperature. Lower part: time−absorption profiles of the spectra shown above at 840 nm.

layer.[11,48] Thus, the PV properties of the SWNT−ZnPc **5** derivative were characterized by using a photoelectrochemical cell; see Figure 8. For the sake of simplicity the photoelectrode consisted of an ITO substrate covered with the SWNT derivative film. The film preparation was handled by filtration and lamination methods[59–64] using suspensions of *p*-SWNTs **6**, *f*-SWNTs **8**, and SWNT−ZnPc **5**. In particular, 0.12 mg of each sample was suspended in 4.8 mL of *o*-dichlorobenzene. These suspensions were diluted to 50 mL before filtering them through a PTFE membrane filter (Millipore, 200 nm pore size, 37 mm diameter). As the solvent passed through the pores, the SWNT samples were trapped on the membrane surface, thereby forming a homogeneous brown layer. Adjusting the initial concentration helps to create conductive films of different optical thickness. In fact, *p*-SWNTs **6**, *f*-SWNTs **8**, and SWNT−ZnPc **5** physical thicknesses were adjusted to provide similar optical transparencies in the spectral range of interest: ranging from 38% to 60% between 300 and 800 nm; see Figure S4.

Before transfer of the films onto ITO-covered glass slides, the latter were first refluxed for 24 h in 2-propanol to render them hydrophobic. They were then pressed on top of the purified SWNTs **6**, *f*-SWNTs **8**, and SWNT−ZnPc **5** films utilizing clamps before the whole assembly was placed in an oven at 130 °C for 20 min. After removal of the sample from the oven, the filter was peeled off, leaving the brown, transparent films on the ITO substrate.

Insight into the film morphology came from AFM and SEM measurements. SEM investigations of *p*-SWNTs **6**, *f*-SWNTs **8**, and SWNT−ZnPc **5** show that the SWNTs homogeneously cover the substrate surface and form a membrane-like film; Figure S5. The SWNTs arrange in intertwined bundles with widths and lengths of around 10 nm and several hundreds of nanometers, respectively. AFM images, not shown, corroborate those observations and in particular the presence of thicker bundles on the surface.

Since photooxidation of the ZnPc was expected under illumination, ascorbic acid was added to the electrolyte solution (0.1 M Na_3PO_4) as a sacrificial electron donor. In addition this should favor anodic currents, because direct injection of electrons from the ascorbate into the ITO conduction band can be expected under positive potential. The presence of ascorbate is essential since in its absence no notable photocurrents arose.

In first sets of experiments, photocurrents were determined for *p*-SWNTs **6**, *f*-SWNTs **8**, and SWNT−ZnPc **5** in the absence and presence of an external bias under white-light illumination. The electrochemical cell consists of three electrodes, SWNT−modified ITO, Pt wire, and Ag/AgCl electrodes, dipped in an electrolyte solution of 0.1 M Na_3PO_4 containing ascorbic acid 5 mM. A simplified representation of the cell is given in Figure 8.

As a first result we observed that the photocurrents were about 30% higher for SWNT−ZnPc **5** than for *p*-SWNTs **6** and *f*-SWNTs **8** under short circuit conditions. A positive photocurrent was always observed in those short circuit conditions,

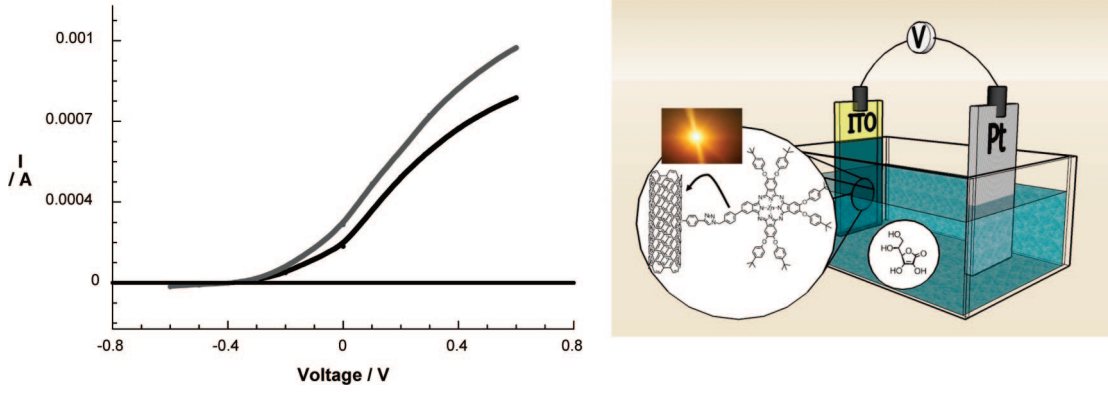

Figure 8. I−V characteristics of SWNT−ZnPc **5** under white light illumination, gray line, and in the dark, black line. Three-electrode setup, 0.1 M Na_3PO_4, 1 mM sodium ascorbate, N_2 purged. Voltages measured versus a Ag/AgCl reference electrode (0.1 M KCl). On the right: schematic representation of the photoelectrochemical cell used for the measurements.

Chart 1

$$\text{ZnPc-SWNT} + h\nu \Rightarrow (\text{ZnPc})^{*}\text{-SWNT}$$

$$(\text{ZnPc})^{*}\text{-SWNT} \Rightarrow (\text{ZnPc})^{\bullet+}\text{-}(\text{SWNT})^{\bullet-}$$

$$(\text{ZnPc})^{\bullet+}\text{-}(\text{SWNT})^{\bullet-} + \text{ITO} \Rightarrow (\text{ZnPc})^{\bullet+}\text{-SWNT} + \text{ITO}^{\bullet-}$$

$$(\text{ZnPc})^{\bullet+}\text{-}(\text{SWNT}) + \text{sacrificial electron donor} \Rightarrow \text{ZnPc-SWNT} + (\text{sacrificial electron donor})^{\bullet+}$$

which is indicative of photogenerated electrons that flow from the film to the ITO electrode. Current−voltage measurements were then carried out in a voltage range between −0.6 V and +0.6 V versus Ag/AgCl (0.1 M KCl). As shown in Figure 8, around −0.4 V an open circuit voltage sets in, where no appreciable currents, neither in the dark nor under illumination, flow. Increasing the bias toward the anodic range resulted in an increase of photocurrent as a consequence of a facilitated electron injection into ITO. These observations are consistent with the expected photooxidation of ZnPc and the presence of ascorbate in the electrolyte. At the maximum applicable bias, prior to performing any irreversible changes in the photoactive layer, the net currents, calculated by subtracting the dark currents from the photocurrents, were 0.22 mA for SWNT−ZnPc **5**. We noticed that the sign of the photocurrent reverted when applying cathodic biases below −0.4 V. However, the current level remained very small corresponding to a very ineffective photocathodic mechanism. This is very likely due to the use of a sacrificial electron donor (i.e., ascorbic acid) in the electrolyte solution, which fail in closing the circuits between the photoelectrode and the Pt counter electrode. Hypothetically, electron acceptors such as methylviologen or O_2 should render this pathway much more efficient. The mechanism for the photoinduced electron transfer in the photoelectrochemical is shown in Chart 1. Next, the photoaction spectra under monochromatic conditions were recorded (Figure 9). In line with what has been noted in the absorption spectra of *p*-SWNTs **6**, *f*-SWNTs **8**, and SWNT−ZnPc **5** on quartz substrates, broad and featureless transitions emerge in the photoaction spectrum between 300 and 800 nm (see Figure S4). Contributions in the near-infrared, that is, operating with a "800 nm" cutoff filter are 13.6%. Finally, the internal photoconversion efficiencies (IPCE) of SWNT−ZnPc **5** were determined. At +0.6 V we derived IPCE values of 17.3% for SWNT−ZnPc **5** (the IPCE for *f*-SWNTs **8** were more than 50% less).

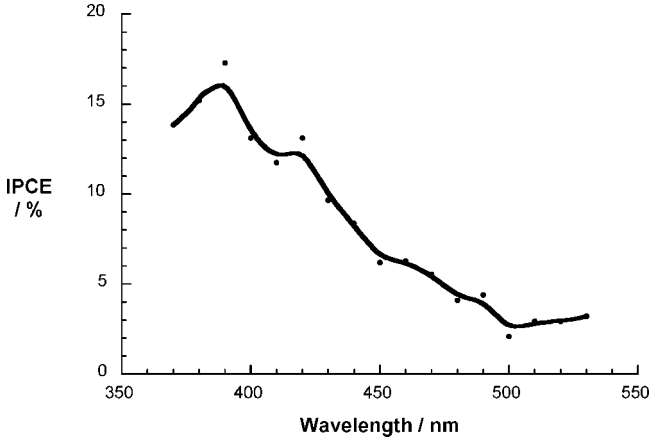

Figure 9. Photoaction spectrum of SWNT−ZnPc **5** recorded with a bias of 0.6 V versus Ag/AgCl (0.1 M KCl).

Conclusions

Here we have described the functionalization of carbon nanotubes with a 4-ethynylbenzene derivative and the subsequent attachment of phthalocyanine molecules using the Huisgen 1,3-dipolar cycloaddition.[32] The nanotube derivatives were fully characterized by a combination of analytical techniques. Photophysical measurements let us identify a photoinduced communication between the two components (i.e., SWNT and ZnPc moieties). Inspired by such unique charge transfer features, we integrated SWNT−ZnPc **5** into photoactive electrodes (i.e., photoanodes), using ITO as a transparent semiconductor, which revealed stable and reproducible photocurrents with monochromatic IPCE values as large as 17.3%.

We have demonstrated that click chemistry is an elegant method to functionalize carbon nanotubes. This concept will be extended to the attachment of other photo- and/or electroactive moieties on carbon nanotubes. Our interest is to produce optoelectronic devices based on functionalized carbon nanotube field effect transistors (*f*CNT-FETs).[20]

Acknowledgment. This work was carried out with the partial support from the University of Trieste, INSTM, and MUR (cofin. Prot. 2006034372 and Firb RBNE033 KMA), SFB 583, DFG (GU 517/4-1), FCI, and the Office of Basic Energy Sciences of the U.S. Department of Energy. Funding from MEC (CTQ2005-08933/BQU and CONSOLIDER-INGENIO 2010 CDS2007-00010 NANOCIENCIA MOLECULAR), COST Action D35, and Comunidad de Madrid (S-0505/PPQ/000225) is acknowledged. We also thank Dr. Oliver Jost (Dresden University), for providing the SWNTs.

Supporting Information Available: Techniques, experimental details, and characterization for the synthesis of phthalocyanine derivatives and functionalization of carbon nanotubes. This material is available free of charge on the World Wide Web at http://pubs.acs.org.

JA8033262

(59) Granstrom, M.; Petritsch, K.; Arias, A. C.; Lux, A.; Andersson, M. R.; Friend, R. H. *Nature* **1998**, *395*, 257.
(60) Wu, Z.; Chen, Z.; Du, X.; Logan, J. M.; Sippel, J.; Nikolou, M.; Kamaras, K.; Reynolds, J. R.; Tanner, B. D.; Hebard, A. F.; Rinzler, G. A. *Science* **2004**, *305*, 1273.
(61) Bernards, D. A.; Flores-Torres, S.; Abruna, H. D.; Malliaras, G. G. *Science* **2006**, *313*, 1416.
(62) Yim, K.-H.; Zheng, Z.; Liang, Z.; Friend, R. H.; Huck, Wilhelm T. S.; Kim, J.-S. *Adv. Funct. Mat.* **2008**, *18*, 1012.
(63) Huang, J.; Li, G.; Yang, Y. *Adv. Mat.* **2008**, *20*, 415.
(64) Kim, J.; Khang, D.-Y.; Kim, Ju-H.; Lee, H. H. *Appl. Phys. Lett.* **2008**, *92*, 133307/1.